Collective-resonance fluorescence in an ideal cavity

H. M. Castro-Beltran,[1] J. J. Sanchez-Mondragon,[1] and S. M. Chumakov[2]
[1]*Instituto Nacional de Astrofísica, Optica y Electrónica, Apartados Postales 51 y 216, 72000 Puebla, Puebla, Mexico*
[2]*Instituto de Investigaciones en Matemáticas Aplicadas y en Sistemas, Universidad Nacional Autónoma de México, Apartado Postal 139-B, 62191 Cuernavaca, Morelos, Mexico*
(Received 7 July 1995; revised manuscript received 27 December 1995)

We study cooperative properties of the emission spectrum of A two-level atoms interacting with a quantized field in a lossless cavity. We show, in a unified treatment, the system anharmonicity, the fine structure, and size of the spectral bands. Further, we show that for an initially inverted atomic system and a thermal cavity field the atomic cooperativity allows the merging of well-defined sidebands, absent in the single-atom case. Thus the cooperativity reduces the destructive effect of the large dispersion of the blackbody photon distribution. For an increasing number of atoms, the central band is split into a doublet. The dip in the doublet is filled when the cavity field is very strong. Also, the extra sidebands have smaller amplitudes than the time-dependent contributions to the spectrum.

PACS number(s): 42.50.Fx, 32.70.Jz

I. INTRODUCTION

The interaction of atoms with blackbody radiation leads generally to irregular dynamics of the system observables, reflecting the large fluctuations of the field. For example, the revivals of the atomic inversion [2,3] and of photon correlations [4] are broader in the presence of thermal photons than in the case of pure coherent field [5]. Particularly interesting are those interactions in the cavity QED frame where coherent quantum effects are stronger than the influence of thermal fluctuations [1]. So far, experiments with high-Q cavities count with a finite number of thermal photons [6,7].

However, it has been shown that atomic collectivity can overcome the thermal fluctuations, as in the observation of coherentlike revivals of the atomic inversion of many atoms interacting with a weak thermal cavity field [3,7,8], along with narrowing of the photon distribution at certain times [8]. This can be explained by the suppression of the large fluctuations of the thermal field due to the coherence of the atomic system.

The resonance fluorescence (RF) spectra from two-level atoms interacting with quantized fields in high-Q cavities also show very interesting features. The weak-field spectrum shows the so-called vacuum Rabi splitting [9,10]. For the case of strong coherent field the spectrum [9,11] resembles the semiclassical one-atom Mollow triplet [12]. While the weak-field spectrum is not very sensitive to the initial field statistics, well suited to testing the radiation discreteness [13], for strong thermal fields the sidebands become very weak and almost flat for one atom [11], and even for two atoms [14], due to the broad photon distribution.

For cooperative RF, the existence of $A-1$ pairs of sidebands (where A is the number of atoms), in addition to the Mollow-like triplet, has been predicted [15,16]. However, these sidebands are very small and difficult to observe experimentally. On the other hand, it has been shown that in a lossless cavity the central band grows linearly, while the sidebands grow quadratically with A [17]. It is to be compared to the free space case, where the three components grow as A^2, keeping the one-atom spectral shape [15,18]. This different behavior suggests that the sidebands would stand out notably against the central band for a large number of atoms.

Indeed, we show in this paper that the coherence provided by an initially inverted atomic system can lead to high spectral sidebands even if the average number of thermal photons in the cavity is significantly larger than the number of atoms. Furthermore, in the strong quantum field case we observe the splitting of the central band with increasing number of atoms due to the lack of an elastic peak. This splitting appears in both the coherent and thermal cases. We also describe the fine structure of the spectral bands for the case of initial Fock field states. These two effects are not a consequence of the given initial photon distribution. It is a fundamental feature of a quantum field interacting with a cooperative atomic system; it disappears in the classical field limit.

We use the perturbation method devised by Kozierowski, Chumakov, and Mamedov [19], based on a SU(2) group representation technique and the approximate dynamical symmetry of the Dicke model, with expansion parameter equal to the inverse square of the Rabi frequency. This method has proved its usefulness in studies of cooperative spontaneous emission [19]. Its advantages are the clear presence of anharmonicity in the eigenfrequencies in a simple analytical form, and ease of calculation of observables. With our model we can obtain the intensities and positions of the $2A+1$ spectral bands, but the extra sidebands are very small in the strong-field region. They are of the same order as transient effects, usually neglected through the secular approximation; hence they are not the best collective spectral features to look at.

We proceed as follows. In Sec. II we explain our model and in Sec. III we calculate the spectrum for an initial Fock, coherent, and thermal fields. In Sec. IV we estimate and compare the linewidths for coherent and thermal fields, and we give our conclusions in Sec. V. Finally, a brief account of our perturbation method is given in the Appendix.

II. THEORETICAL MODEL

We use the model originally proposed by Dicke [20]. It considers a system of A identical two-level atoms interacting

resonantly with a single mode of a quantized field of frequency ω in a lossless cavity. We neglect direct interatomic forces, and assume that all atoms have equivalent mode positions, having therefore the same coupling constant g. The rotating-wave approximation Dicke model [20] Hamiltonian has the form ($\hbar=1$):

$$\mathscr{H}=\omega(a^{\dagger}a+L^{Z})+g(aL^{+}+a^{\dagger}L^{-}), \tag{1}$$

where $a^{\dagger}$ and a are the photon creation and annihilation operators, and the collective atomic operators are described by

$$\begin{aligned} &L^{+}|m\rangle_a=\sqrt{(m+1)(A-m)}\,|m+1\rangle_a,\\ &L^{-}|m\rangle_a=\sqrt{m(A-m+1)}\,|m-1\rangle_a,\\ &L^{Z}|m\rangle_a=\left(m-\frac{A}{2}\right)|m\rangle_a,\\ &L^{X}=(L^{+}+L^{-})/2,\quad L^{Y}=(L^{+}-L^{-})/2i, \end{aligned} \tag{2}$$

where $|m\rangle_a$ is the symmetric atomic state with m excited atoms. The atomic operators generate the $(A+1)$-dimensional representation of the SU(2) group.

Dicke stressed the role of the symmetry of the initial atomic state under permutations of atoms and found the states that lead to enhanced spontaneous emission (superradiance). Tavis and Cummings [21] reformulated this problem in matrix form and reduced the problem to solving an algebraic equation of a high degree. The early computer experiments showed that there exist regimes where the spectrum of the model is nearly linear [22]. Correspondingly, the early analytical papers [23–25] considered the linearized versions of the problem. For instance, Bonifacio and Preparata [26] and Kumar and Mehta [27] presented approximate solutions for the time evolution of the atomic inversion in terms of elliptic functions (compare the later paper [28]). It has become clear now that anharmonic phenomena due to the nonlinearity of the model become especially important if we treat the field as a quantum object (see, e.g., [29]). It can be easily understood in the one-atom case [30], where in the linear approximation we get the Rabi oscillations of the atomic inversion, but not the collapses and revivals of these oscillations. The goal of recent work [31,32] was to investigate the nonlinear corrections to the spectrum (i.e., to solve the algebraic equation of the high degree mentioned above). We shall use here the approach based on the approximate dynamical symmetry of the Dicke model [19]. To our knowledge, it is the only solution available in a closed and simple form, which can be used to calculate the physical properties of the model in different dynamical regimes; see [19].

To write down the solution, we need to introduce some notation. Let us recall that the excitation number operator, $\mathscr{N}=a^{\dagger}a+L^{Z}+A/2$, commutes with the Hamiltonian (1). We are interested here in the strong-field regime, where the number of atoms is less than the excitation number N. Then the dynamics is restricted to a $(A+1)$-dimensional subspace, spanned by the ''bare'' basis

$$|N,m\rangle=|N-m\rangle_f\otimes|m\rangle_a,\quad 0\leqslant m\leqslant A. \tag{3}$$

Here $|n\rangle_f$ is the Fock field state with n photons. It is convenient to work in a dressed system basis, labeling the eigenvectors and eigenvalues by the indices N and p, $0\leqslant p\leqslant A$. We write the eigenvalue equations for the interaction Hamiltonian $\mathscr{V}=g(aL^{+}+a^{\dagger}L^{-})$ and the excitation number operator as

$$\mathscr{V}|\Psi_{N,p}\rangle=\Lambda_p^N|\Psi_{N,p}\rangle,\quad \mathscr{N}|\Psi_{N,p}\rangle=N|\Psi_{N,p}\rangle. \tag{4}$$

Then the evolution operator is given in terms of the dressed vectors by

$$U(t)=\sum_{p=0}^{A}|\Psi_{N,p}\rangle e^{-i(\Lambda_p^N+\omega N)t}\langle\Psi_{N,p}|. \tag{5}$$

It is well known that the energy spectrum is not equidistant for an arbitrary number of atoms [22]. From the perturbation theory shown in the Appendix, the approximate eigenvalues and eigenvectors are

$$\Lambda_p^N=(A-2p)\Omega_N\left\{1-\frac{g^4}{32\Omega_N^4}[10p(A-p)-(A-1)(A-2)]\right\}, \tag{6}$$

$$|\Psi_{N,p}\rangle=|\underline{N,p}\rangle+\frac{g^2}{8\Omega_N^2}[(A-2p+1)\sqrt{p(A-p+1)}\,|\underline{N,p-1}\rangle-(A-2p-1)\sqrt{(p+1)(A-p)}\,|\underline{N,p+1}\rangle], \tag{7}$$

where

$$\Omega_N=g\sqrt{N-A/2+1/2} \tag{8}$$

is the collective Rabi frequency, and $|\underline{N,p}\rangle$ are the lowest (zeroth-) order eigenvectors, whose components are given by

$$\alpha_{mp}=\langle N,m|\underline{N,p}\rangle=\sqrt{\frac{m!p!}{2^A(A-m)!(A-p)!}}\sum_{j=0}^{\min(m,p)}\frac{(-2)^j(A-j)!}{j!(m-j)!(p-j)!}. \tag{9}$$

The first-order eigenvectors, Eq. (7), can be rewritten in terms of α_{mp} as

$$\mathscr{A}_{mp}^N=\langle N,m|\Psi_{N,p}\rangle=\alpha_{mp}+\frac{g^2}{8\Omega_N^2}[(A-2p+1)\sqrt{p(A-p+1)}\,\alpha_{m,p-1}-(A-2p-1)\sqrt{(p+1)(A-p)}\,\alpha_{m,p+1}]. \tag{10}$$

The matrix $\mathscr{A}$ describes the transformation between the bare and the dressed vectors, i.e., $|\Psi_{N,p}\rangle=\mathscr{A}|N,m\rangle$. In zeroth order, $\mathscr{A}\to\alpha$ and $|\underline{N,p}\rangle=\alpha|N,m\rangle$. As one can see from Eq. (6), the first-order corrections to the eigenvalues always vanish. Moreover, for $A=1$ all the higher-order corrections vanish and in zeroth order we recover the exact expressions for the Jaynes-Cummings model [33]. The matrix α diagonalizes the zeroth-order Hamiltonian $\mathscr{V}_0=2gL^{X}$ (see Appen-

dix), $\alpha L^X \alpha = L^Z$. Note that $\Sigma_{p=0}^{A} \alpha_{mp}^2 = 1$. Moreover, α does not depend on N. It is convenient to introduce also the rotated operators $\alpha L^{\pm} \alpha = X^{\pm}$. They are connected with the operators $L^{\pm}, L^X$ as follows:

$$L^{\pm} = L^X \pm \tfrac{1}{2}(X^- - X^+), \quad L^Z = \tfrac{1}{2}(X^- + X^+). \tag{11}$$

The matrix elements of these new operators in the basis of the zeroth-order eigenvectors $|\underline{N,p}\rangle$ have a very simple form:

$$\begin{aligned} \langle \underline{N-1,q}|L^X|\underline{N,p}\rangle &= \tfrac{1}{2}(A-2p)\,\delta_{qp}, \\ \langle \underline{N-1,q}|X^-|\underline{N,p}\rangle &= \sqrt{p(A-p+1)}\,\delta_{qp-1}, \\ \langle \underline{N-1,q}|X^+|\underline{N,p}\rangle &= \sqrt{(p+1)(A-p)}\,\delta_{qp+1}. \end{aligned} \tag{12}$$

Therefore, the operators $X^{\pm}$ shift up and down the eigenvectors of L^X. Now, in order to calculate the matrix elements of any atomic operator, we may first express it in terms of the operators $X^{\pm}, L^X$ by means of Eqs. (11) and then make use of Eqs. (12). Below we shall use the following matrix elements:

$$\begin{aligned} \langle \underline{N-1,q}|L^-|\underline{N,p}\rangle = \left(\frac{A}{2}-p\right)\delta_{q,p} + \frac{1}{2}\sqrt{(p+1)(A-p)}\,\delta_{q,p+1} \\ - \frac{1}{2}\sqrt{p(A-p+1)}\,\delta_{q,p-1}. \end{aligned} \tag{13}$$

III. COLLECTIVE EMISSION SPECTRA

In this section we obtain an analytic expression for the Dicke model RF spectrum in terms of Fock states of the field and use it to find the spectrum for thermal and coherent fields. The standard definition of the physical spectrum [34] is

$$\begin{aligned} S(\nu,t) \equiv 2\gamma \int_0^t dt_1 \int_0^t dt_2 e^{-(\gamma - i\nu)(t-t_2)} \\ \times e^{-(\gamma + i\nu)(t-t_1)} G(t_1,t_2), \end{aligned} \tag{14}$$

where γ and ν are the filter bandwidth and peak transmission frequency, respectively, and $G(t_1,t_2)$ is the two-time collective dipole correlation function:

$$\begin{aligned} G(t_1,t_2) &= \langle L^+(t_2) L^-(t_1)\rangle \\ &= \sum_n P_{nf} \langle n|_a \langle m|U^\dagger(t_2) L^+ U(t_2) \\ &\quad \times U^\dagger(t_1) L^- U(t_1)|n\rangle_f |m\rangle_a \\ &= \sum_{n=0}^{\infty} P_n \sum_{p,q,r=0}^{A} \mathscr{A}_{mp}^N \overline{\mathscr{A}}_{mr}^N e^{i(\omega + \omega_{qp}^N)t_2} \\ &\quad \times e^{-i(\omega + \omega_{qr}^N)t_1} \langle \Psi_{N,p}|L^+|\Psi_{N-1,q}\rangle \\ &\quad \times \langle \Psi_{N-1,q}|L^-|\Psi_{N,r}\rangle. \end{aligned} \tag{15}$$

Here $|m\rangle_a$ is the initial state of the atomic system, P_n is the initial photon probability distribution, and $\omega_{qp}^N \equiv \Lambda_p^N - \Lambda_q^{N-1}$ are the frequencies of the spectral components. To obtain the second equality we have used Eq. (5). After the filter integration and passing the transient process, $\gamma t > 1$, we get

$$\begin{aligned} S(\Delta_f,t) = 2\gamma \sum_{N=m}^{\infty} P_{N-m} \sum_{p,q,r=0}^{A} \mathscr{A}_{mp}^N \overline{\mathscr{A}}_{mr}^N \\ \times \langle \Psi_{N,p}|L^+|\Psi_{N-1,q}\rangle \langle \Psi_{N-1,q}|L^-|\Psi_{N,r}\rangle \\ \times \frac{\exp[it(\omega_{qr}^N - \omega_{qp}^N)]}{[\gamma - i(\Delta_f - \omega_{qr}^N)][\gamma + i(\Delta_f - \omega_{qp}^N)]}, \end{aligned} \tag{16}$$

with $\Delta_f = \nu - \omega$ being the filter-field detuning. Note that the summation over the initial photon number n in Eq. (15) has been transformed into a summation over the initial excitation number $N = n + m$ in Eq. (16). For $p \neq r$ we have oscillatory terms that contain the product of two complex Lorentzians, peaked at ω_{qr}^N and ω_{qp}^N, so that the oscillation amplitudes are small. They are of the order of $1/\Omega_N$. Here we shall consider only the time-independent part of the spectrum, which is given by the terms $p = r$. We have a real Lorentzian for every value of p and q,

$$S(\Delta_f) = 2\gamma \sum_{N=0}^{\infty} \sum_{q,p=0}^{A} P_{N-m} \frac{|\mathscr{A}_{mp}|^2 |\langle \Psi_{N-1,q}|L^-|\Psi_{N,p}\rangle|^2}{\gamma^2 + (\Delta_f - \omega_{qp}^N)^2}. \tag{17}$$

This equation gives the stationary physical spectrum in terms of the system eigenvalues and eigenvectors. To continue we need to calculate them numerically or use some analytical approximation. We choose to use the approximations (6) and (7) since they give us better insight into the physics of the process. (Computer simulations with exact eigenvalues and eigenvectors show a full agreement with our analytical treatment.)

It is very instructive to start with the case of an initial Fock field state [the term with a given value of $N = n + m$ in the external sum of Eq. (17)]. The eigenvalues (6) determine the positions of the spectral components. Denoting $q = p + k$, we have

$$\begin{aligned} \omega_{p+k,p}^N = 2k\Omega_N + \frac{g^2}{\Omega_N}(A/2 - k - p) + \frac{g^4}{16\Omega_N^3}\{2(A-2p-2k) \\ - k[10p(A-p) + 10k(A-2p-k) \\ - (A-1)(A-2) - 5(A-2p)(A-2p-k)]\}, \end{aligned} \tag{18}$$

where $k = 0$ labels the central band, $k = 1$ (-1) the first right (left) sideband, and so on. Neighboring bands are separated by $2\Omega_N$. The first-order terms give the separation of peaks inside a band, g^2/Ω_N. The second-order terms give the finest corrections to the peak positions. The p index numerates the peaks inside a given band and goes as $0 \leq p \leq A$ for the central band, $0 \leq p \leq A-1$ for the first right sideband, and $1 \leq p \leq A$ for the first left sideband. For $-A \leq k \leq A$ there are $2A+1$ bands, and the number of peaks in the kth band is $A + 1 - |k|$. For even A one peak disappears in the central band, the elastic peak, so that it consists of A peaks for even A and of $A+1$ peaks for odd A; see Eqs. (20) below. Kien, Shumovsky, and Quang [16] predicted the eight peak total

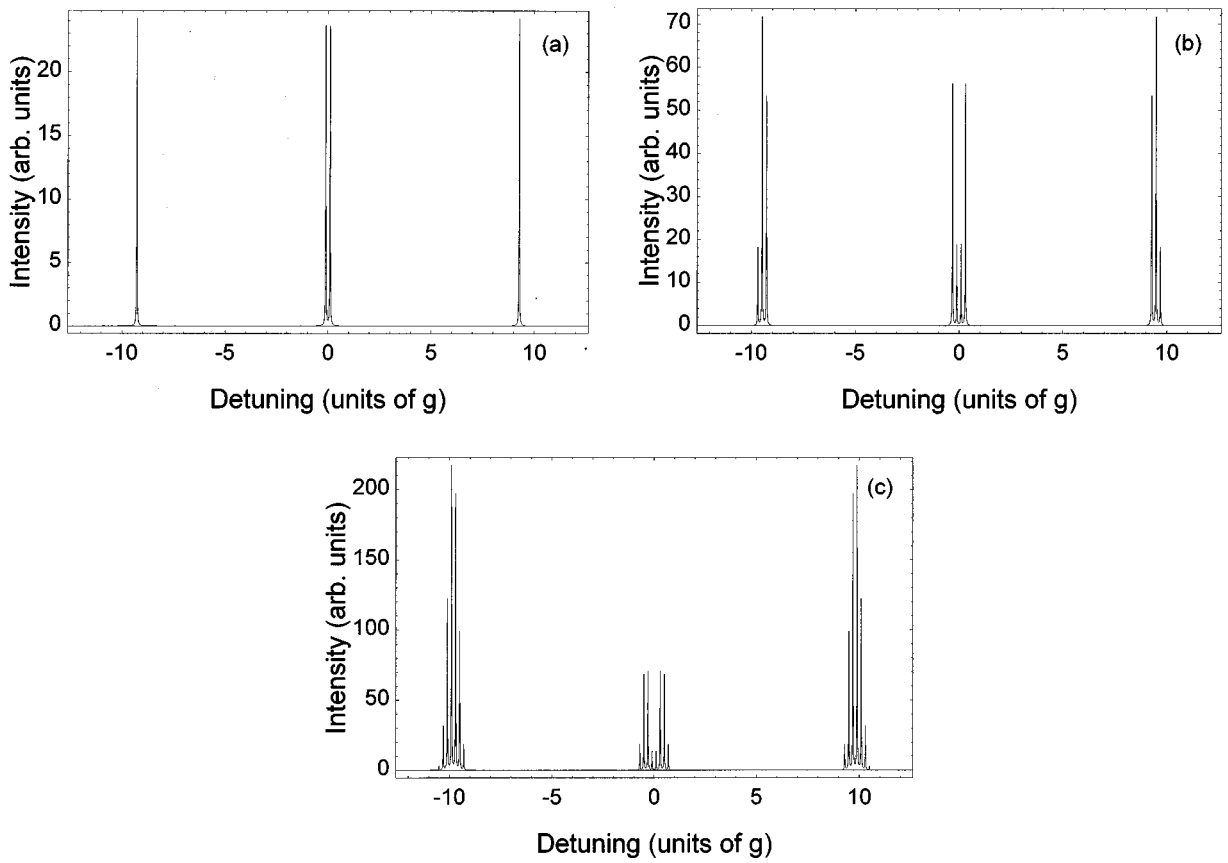

FIG. 1. Fine structure and relative intensities of the spectral bands vs filter detuning $\Delta_f=\nu-\omega$ in units of the coupling constant g, for a field in the number state $n=21$ and (a) $A=1$ (Jaynes-Cummings model spectrum), (b) $A=3$, and (c) $A=7$. All the atoms are initially excited, $m=A$. Filter bandwidth $\gamma=0.01g$.

spectrum for the two-atom case. We conclude that the spectrum has *cooperative fine structure* if the field is in a number state.

The coefficients

$$I_{qp}=|\mathscr{A}_{mp}|^2|\langle\Psi_{N-1,q}|L^-|\Psi_{N,p}\rangle|^2 \tag{19}$$

determine the intensities of the spectral lines. For the special case of having all the atoms initially in the same (ground or excited) state, $m=0,A$, the zeroth-order amplitudes $|\alpha_{mp}|^2$ are proportional to the binomial coefficients [it follows from Eq. (9)]. Then, from Eq. (13) we obtain the distribution of peak intensities in every band of the basic triplet,

$$I_{p+1,p}=\frac{A!}{(A-p)!p!}\frac{(p+1)(A-p)}{2^{A+2}},$$

$$I_{p,p}=\frac{A!}{(A-p)!p!}\frac{(A-2p)^2}{2^{A+2}},$$

$$I_{p-1,p}=\frac{A!}{(A-p)!p!}\frac{p(A-p+1)}{2^{A+2}}, \tag{20}$$

for the right, central, and left bands, respectively (Fig. 1). The most outstanding effect of cooperativity is in the size of the sidebands compared to the central band. Performing the sum of each of Eqs. (20) over the p states, the central to sideband integrated intensity ratio is

$$I_0:I_{\pm1}\rightarrow\frac{A}{4}:\frac{A(A+1)}{16}, \tag{21}$$

a result obtained by Shumovsky and Quang [17] in a semiclassical treatment. They noticed the linear dependence on A of the central band in a cavity compared to the A^2 result for free space, in which case the strong-field spectral line shape approaches that for one atom [15,18]. We can see that $I_{\pm1}\geqslant I_0$ for $A\geqslant3$.

The extra sidebands are very small in the strong field region. The kth band appears in the $(k-1)$th order of the perturbation theory and has the time-independent intensity proportional to $\Omega_n^{-4(k-1)}$. Hence the extra sidebands are smaller than the oscillatory contributions. For most of what follows we restrict ourselves to a study of the steady triplet spectrum which appears naturally in the zeroth order of our perturbation theory. Thus we neglect the time-dependent part of the spectrum, additional sidebands, and the corrections to the intensity of the triplet. The extra sidebands are also small in the weak-field region, when the number of atoms is larger than the number of photons. They can become important only if $A\sim\overline{n}$. In the remainder of the paper we only consider the case of initially excited atomic system, $m=A$.

The final height and shape of the spectral bands are marked by the initial photon statistics. The thermal and coherent fields are represented by the blackbody and Poisson distributions,

$$P_n^{\rm th}=\frac{\overline{n}^n}{(1+\overline{n})^{n+1}},\quad P_n^{\rm coh}=\frac{e^{-\overline{n}}\overline{n}^n}{n!},\tag{22}$$

whose dispersions Δn are given by $\sqrt{\overline{n}(\overline{n}+1)}$ and $\sqrt{\overline{n}}$, respectively, where $\overline{n}$ is the appropriate average photon number. The high coherent-field-induced ''Poisson'' spectrum and the broad asymmetric ''thermal'' sidebands are the most evident aspects when comparing spectra, as seen in Figs. 2–4. As a result of Eq. (21), for an increasing number of atoms the thermal sidebands become clearly defined (Fig. 2), while the Poisson sidebands soon grow higher than the central band (Fig. 3).

On the other hand, the absence of the elastic peak leads to a doublet envelope of the central band, enhanced by large cooperativity, given as the product of the parabolic factor $(A-2p)^2$ and the binomial coefficients in $I_{p,p}$, for every excitation number N. While increasing the field intensity is of little effect on the shape of the Poissonian spectrum, the thermal sidebands become damped and broader (Fig. 4), reflecting the large fluctuations of the blackbody radiation in the cavity. We observe a competition between atomic cooperativity and field properties in the line shape, which we study numerically in the next section.

IV. SPECTRAL LINE SHAPE

The mean position of a band is given by $\overline{\omega_k}=\langle\langle\omega_{p+k,p}\rangle_p\rangle_n$, where the double brackets denote averages over both the p and n state distributions, Eqs. (20) and (22). The terms with $n\sim\overline{n}$ are closer to the resonance (mean) position. For the sidebands in the coherent case

$$(\overline{\omega_{\pm1}})^{\rm coh}\simeq\pm2\overline{\Omega}\mp\frac{Ag^2}{(A+1)\overline{\Omega}}.\tag{23}$$

Here $\overline{\Omega}=g\sqrt{\overline{n}+A/2+1/2}$ is the mean Rabi frequency for $m=A$; see Eq. (8). However, the mean and peak positions of the thermal sidebands do not coincide with $(\overline{\omega_{\pm1}})^{\rm coh}$ being pulled to the center of the spectrum by the low n states of $P_n^{\rm th}$. The large thermal fluctuations renormalize the Rabi frequency but a large number of atoms reduce the resonance shift (Fig. 5), making the interaction more ''coherent.'' Similar thermally induced shifts and asymmetries have been studied in micromaser line shapes [35].

The cooperative fine structure of the bands would be revealed for $\gamma<g^2/\overline{\Omega}$, which is the separation between two neighboring p states, while the separation between the n and $n-1$ photon contributions to a sideband (central band) from a field with a given P_n is $g^2/\overline{\Omega}$ ($g^4/4\overline{\Omega}^3$). We can then neglect the width of the p state distribution of the sideband, but not that for the central band. Both cooperative and photon fine structures are lost if a semiclassical theory is followed. The oscillations in the thermal sidebands in Figs. 2 and 4 ($\gamma=0.25g$) are due to the small-n photon contributions, having small Rabi frequency, which consequently have large separation between two photon number peaks. The large n and the p contributions mix up and erase the fine structure for most of a sideband.

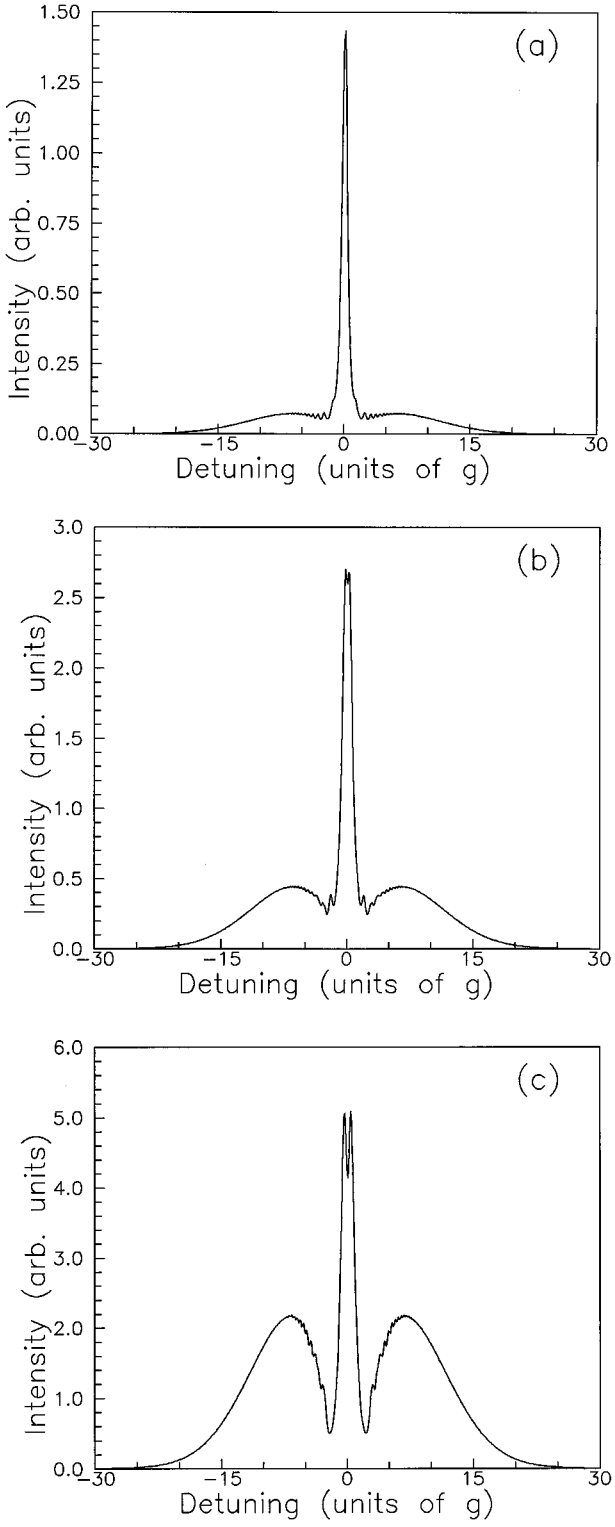

FIG. 2. Collective emission spectra for a thermal field with $\overline{n}=21$ and (a) $A=1$, (b) $A=3$, and (c) $A=7$, for $m=A$ and $\gamma=0.25g$.

The width of the kth band can be computed with the standard formula

$$\sigma_k=\sqrt{\langle\omega_k^2\rangle_n-\langle\omega_k\rangle_n^2},\tag{24}$$

for which we can obtain approximate expressions via

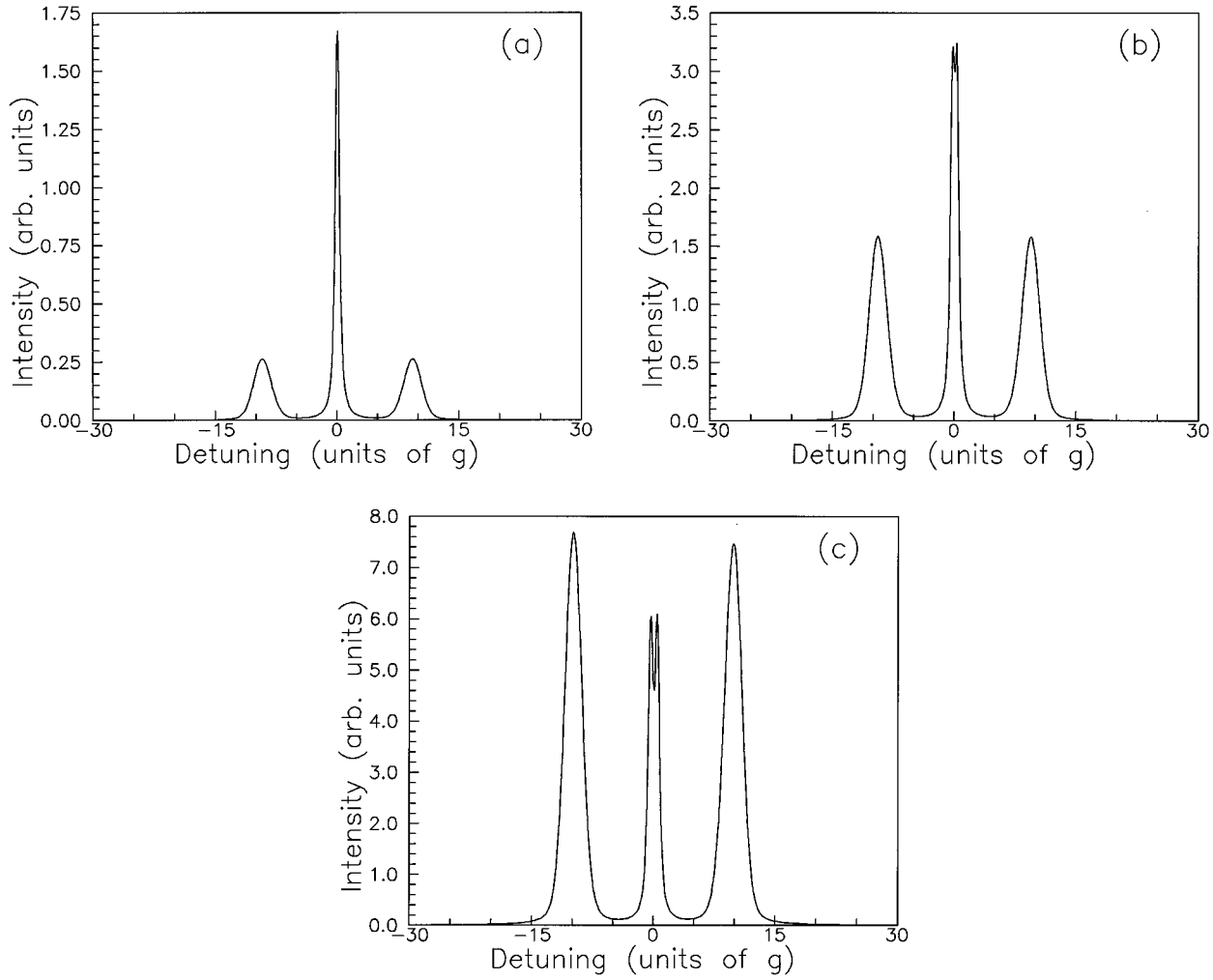

FIG. 3. Same as Fig. 2 for initial coherent field.

$$\sigma_k = \omega_k(\overline{n}+\Delta n) - \omega_k(\overline{n}). \tag{25}$$

For coherent field the approximations are very good, while for a thermal field the approximations are still good. For the sidebands we have

$$\sigma_{\pm 1}^{\mathrm{coh}} \approx \frac{g^2\sqrt{\overline{n}}}{\overline{\Omega}}, \quad \sigma_{\pm 1}^{\mathrm{th}} \approx 2(\sqrt{2}-1)\frac{g^2\overline{n}}{\overline{\Omega}}. \tag{26}$$

For large $\overline{n}$ every n thermal state contributes little to the spectrum, resulting in small and broad sidebands, that is, a strong thermal field acts as damping. The closeness of the central band adds a small amount of broadening to the thermal sideband for A small. Figure 6 shows cooperative narrowing of the sidebands when all atoms are initially excited, more for a thermal than for a coherent field.

The central band shows a dip due to the lack of an elastic peak in the quantum field formulation; the dip becomes wider for increasing atomic cooperativity, Fig. 7. The band envelope is given by $I_{p,p}$, Eq. (20). In general, the central band is less sensitive to the field statistics than the sidebands. The whole band is not completely filled, at least for not very strong fields, due to the much smaller separation of two neighboring n-photon contributions than that of the p states ($g^4/4\overline{\Omega}^3 \ll g^2/\overline{\Omega}$), which explains its reduced sensitivity to the initial P_n. The dip is filled slightly faster with increasing thermal field than with a coherent field due to the larger width of every p peak of the former

$$\sigma_0^{\mathrm{coh}} = \frac{g^4\sqrt{\overline{n}}}{4\overline{\Omega}^3}, \quad \sigma_0^{\mathrm{th}} \approx \frac{g^2}{\sqrt{8}\overline{\Omega}}(\sqrt{2}-1). \tag{27}$$

Note that the cooperative width of the central band (due to the distribution of p states) is

$$\sigma_0^{\mathrm{coop}} = \frac{g^2\sqrt{A}}{2\overline{\Omega}}. \tag{28}$$

As mentioned above, this is larger than the spread due to photon statistics for both coherent and thermal fields.

V. CONCLUSIONS

We have studied collective features of the emission spectrum of many atoms in an ideal cavity. The quadratic growth of the sidebands with the number of atoms A (compared to the linear growth of the central band) and their narrowing when all the atoms are initially inverted, allow the formation

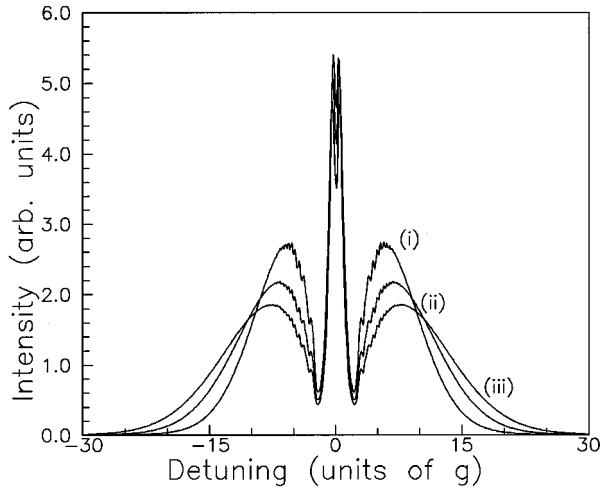

FIG. 4. Effect of damping of a thermal field of increasing intensity on spectra for $A=7$ and (i) $\overline{n}=14$, (ii) $\overline{n}=21$, and (iii) $\overline{n}=28$ (with higher central doublet).

of well-defined sidebands even if a strong thermal field is present in the cavity. Since the Rabi frequency is a sign of coherence in the field-atom interaction, a large number of initially excited atoms would reduce the thermal fluctuations. This suggests that further studies on the competition between atomic coherence and field incoherence be made.

For a quantized cavity field the $A+1$ dressed levels appear, whose positions depend on the initial photon number. This leads to spectral fine structure. The lack of an elastic peak in this case originates a dip in the central band, which is enhanced with an increasing number of atoms. However, this dip is filled in the classical field limit. We have also shown that the steady intensities of the extra sidebands are smaller than the time-dependent (oscillatory) contributions.

Finally, we may note that the vacuum Rabi splitting in the absorption spectra of the collective atomic system in a high-Q cavity has been observed in optical experiments [10,36]. The emission spectra have richer structure, since transitions between many dressed states are involved [37]. Our results, in fact, show that the quantum field features can be seen in emission spectra of a collective atomic system in a good cavity even for coherent and thermal fields of high intensity

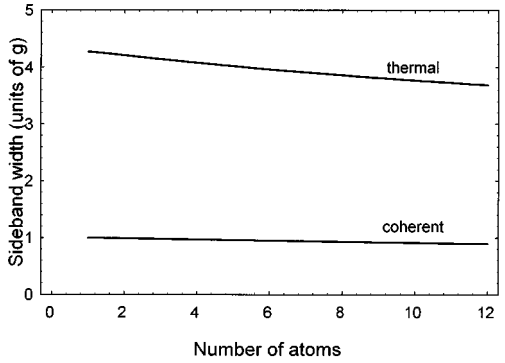

FIG. 6. Width of the sidebands for thermal (upper curve) and coherent field (lower curve) with $\overline{n}=21$.

(for photon numbers much larger than atomic numbers). It seems realistic to observe these phenomena (the high sidebands in comparison with the central band, and the cooperative doublet structure of the central band) both in optical and microwave experiments (see, e.g., [10,38]).

ACKNOWLEDGMENTS

The authors thank Dr. Andrey Klimov, Dr. Maciej Kozierowski, Dr. Erwin Martí-Panameño, and Dr. Héctor Moya-Cessa for many interesting discussions, and Dr. Camilo Arancibia for help with the graphics. H.M.C.B. acknowledges the support of a scholarship from Consejo Nacional de Ciencia y Tecnología, México. S.Ch. is grateful for hospitality to the Instituto Nacional de Astrofísica, Optica y Electrónica, Puebla, Mexico, where this work was performed.

APPENDIX

In this appendix we briefly outline the perturbation theory of Ref. [19], which our RF theory rests on. Note that the theory is expressed here in terms of the strong-field situation, $N>A$. We write the interaction Hamiltonian in the form

$$\mathscr{V}=\mathscr{V}^{+}+\mathscr{V}^{-}, \quad \mathscr{V}^{-}=ga^{\dagger}\sum_{j=1}^{A} L_j^{-}, \quad \mathscr{V}^{+}=ga\sum_{j=1}^{A} L_j^{+}, \tag{A1}$$

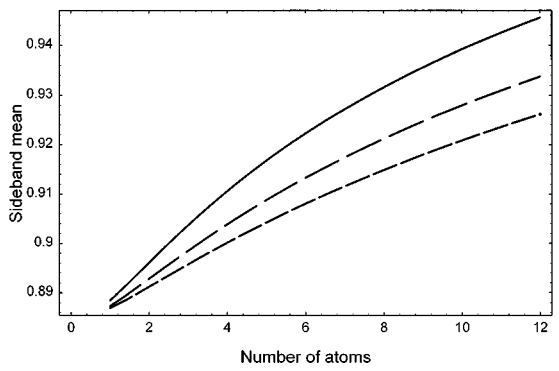

FIG. 5. Normalized mean position of the thermal sideband in units of $\overline{\omega_{k=1}}$ (coherent field). Solid, long-dashed, and short-dashed curves are for $\overline{n}=14$, 21, and 28, respectively.

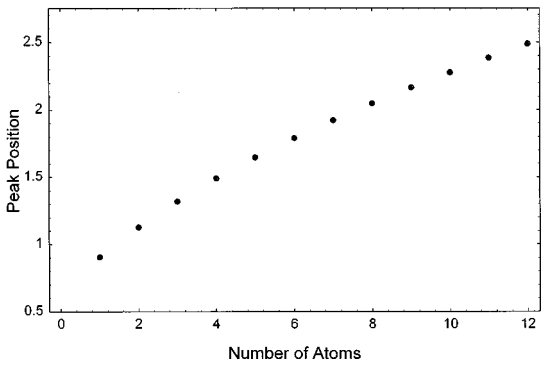

FIG. 7. Distance of the maxima of the distribution $I_{p,p}$ (central doublet) from the center of the spectrum, in units of g^2/Ω as a function of the number of atoms.

with nonvanishing matrix elements

$$\langle N,m-1|\mathscr{V}^{-}|N,m\rangle = g\sqrt{m(A-m+1)(N-m+1)} = \langle N,m|\mathscr{V}^{+}|N,m-1\rangle. \quad \text{(A2)}$$

Expanding in a power series in the parameter $\epsilon = g^2/\Omega_N^2$ we have

$$\langle N,m-1|\mathscr{V}^{-}|N,m\rangle = g\sqrt{\frac{m(A-m+1)}{\epsilon}} \times\left[1+\frac{\epsilon}{2}\left(\frac{A+1}{2}-m\right) -\frac{\epsilon^2}{8}\left(\frac{A+1}{2}-m\right)^2+\cdots\right], \quad \text{(A3)}$$

which requires not only ϵ to be small but $A \ll N$ as well. Actually, the perturbation theory works well even if ϵ and A are not very small.

In this space of $A+1$ dimensions there acts the representation of the SU(2) group, whose generators are L^+, L^-, and L^Z, and the interaction Hamiltonian is expanded as

$$\mathscr{V}^{-} = \sum_{l=0}^{\infty} \epsilon^{l-1/2}\mathscr{V}_l^{-}, \quad \mathscr{V}_l^{-} = gK_l[L^-(\tfrac{1}{2}-L^Z)^l + (\tfrac{1}{2}-L^Z)^l L^+], \quad \text{(A4)}$$

$$K_0=1, \quad K_1=1/2, \quad K_l=(-1)^{l+1}\frac{(2l-3)!!}{2^l l!}, \quad l\geqslant 2. \quad \text{(A5)}$$

In particular we see that $\mathscr{V}_0^{-} = 2gL^X$.

Now we can obtain perturbation expansions that lead to Eqs. (6) and (7):

$$\Lambda_p^N = \frac{g}{\sqrt{\epsilon}}[\lambda_p^{(0)} + \epsilon\lambda_p^{(1)} + \epsilon^2\lambda_p^{(2)} + \cdots], \quad \text{(A6)}$$

$$|\Psi_{N,p}\rangle = \sum_{q=0}^{A} C_{p,q}|\underline{N,q}\rangle, \quad C_{p,q} = C_{p,q}^{(0)} + C_{p,q}^{(1)} + \cdots, \quad \text{(A7)}$$

where $C_{p,q}^{(0)} = \delta_{p,q}$ and $\lambda_p^{(0)} = A-2p$. It is customary to obtain corrections up to second order for eigenvalues and to first order for eigenvectors. By standard perturbation methods we have

$$\lambda_p^{(1)} = \langle \underline{N,p}|\mathscr{V}_1^{-}|\underline{N,p}\rangle,$$
$$\lambda_p^{(2)} = \langle \underline{N,p}|\mathscr{V}_2^{-}|\underline{N,p}\rangle + \sum_{q\neq p,q=0}^{A} \frac{|\langle \underline{N,q}|\mathscr{V}_1^{-}|\underline{N,p}\rangle|^2}{\lambda_p^{(0)}-\lambda_q^{(0)}},$$
$$C_{p,q}^{(1)} = \frac{\langle \underline{N,q}|\mathscr{V}_1^{-}|\underline{N,p}\rangle}{\lambda_p^{(0)}-\lambda_q^{(0)}}. \quad \text{(A8)}$$

With the Hamiltonians $\mathscr{V}_1^{-}$ and $\mathscr{V}_2^{-}$ and Eqs. (11) and (12) we have

$$\langle \underline{N,q}|\mathscr{V}_1^{-}|\underline{N,p}\rangle = -\tfrac{1}{4}[(A-2p+1)\sqrt{p(A-p+1)}\,\delta_{q,p-1} + (A-2p-1) \times\sqrt{(p+1)(A-p)}\,\delta_{q,p+1}],$$

$$\langle \underline{N,q}|\mathscr{V}_2^{-}|\underline{N,p}\rangle = -\tfrac{1}{32}\{(A-2p)[A-1+2p(A-p)]\delta_{q,p} + (A-2p+2) \times\sqrt{(p-1)p(A-p+1)(A-p+2)} \times\delta_{q,p-2} + (A-2p-2) \times\sqrt{(p+1)(p+2)(A-p-1)(A-p)} \times\delta_{q,p+2}\}. \quad \text{(A9)}$$

Then, substituting these results in Eqs. (35) and (34) we obtain Eqs. (6) and (7). Note that the first-order approximation to the eigenvalues vanishes.

[1] For review see, for example, S. Haroche, in *Fundamental Systems in Quantum Optics*, edited by J. Dalibard, J.M. Raimond, and J. Zinn-Justin (Elsevier, Amsterdam, 1992).

[2] P.L. Knight and P.M. Radmore, Phys. Lett. **90A**, 342 (1982); G. Arroyo-Correa and J.J. Sanchez-Mondragon, Quantum Opt. **2**, 409 (1990).

[3] S.M. Barnett and P.L. Knight, Opt. Acta **31**, 1203 (1984).

[4] R.R. Puri and A. Joshi, Opt. Commun. **69**, 367 (1989).

[5] N.B. Narozhny, J.J. Sanchez-Mondragon, and J.H. Eberly, Phys. Rev. A **23**, 236 (1981).

[6] D. Meschede, H. Walther, and G.M. Muller, Phys. Rev. Lett. **54**, 551 (1985); G. Rempe, H. Walther, and N. Klein, *ibid.* **58**, 353 (1987).

[7] J.M. Raymond, P. Goy, M. Gross, C. Fabre, and S. Haroche, Phys. Rev. Lett. **49**, 17 (1982); **49**, 1924 (1982); Y. Kaluzny, P. Goy, M. Gross, J.M. Raymond, and S. Haroche, *ibid.* **51**, 1175 (1983).

[8] S.M. Chumakov and J.J. Sanchez-Mondragon, Opt. Commun. **107**, 231 (1994).

[9] J.J. Sanchez-Mondragon, N.B. Narozhny, and J.H. Eberly, Phys. Rev. Lett. **51**, 550 (1983); J. J. Sanchez-Mondragon, Ph.D. thesis, University of Rochester, 1980 (unpublished).

[10] M.G. Raizen, R.J. Thompson, R.J. Brecha, H.J. Kimble, and H.J. Carmichael, Phys. Rev. Lett. **63**, 240 (1989); R.J. Thompson, G. Rempe, and H.J. Kimble, *ibid.* **68**, 1132 (1992).

[11] J. Gea-Banacloche, R.R. Schlicher, and M.S. Zubairy, Phys. Rev. A **38**, 3514 (1988).

[12] B.R. Mollow, Phys. Rev. **188**, 1969 (1969).

[13] G.S. Agarwal, R.K. Bullough, and N. Nayak, Opt. Commun. **85**, 202 (1991); J.I. Cirac, H. Ritsch, and P. Zoller, Phys. Rev. A **44**, 4541 (1991); L. Tian and H.J. Carmichael, Quantum Opt. **4**, 131 (1992).

[14] T. Maqbool and M.S.K. Razmi, J. Opt. Soc. Am. B **10**, 112 (1993).

[15] I.R. Senitzky, Phys. Rev. Lett. **40**, 1334 (1978); H.J. Carmichael, *ibid.* **43**, 1106 (1979); P.D. Drummond and S.S. Hassan, Phys. Rev. A **22**, 662 (1980); G.S. Agarwal, R. Saxena, L.M. Narducci, D.H. Feng, and R. Gilmore, *ibid.* **21**, 257 (1980).
[16] F.L. Kien, A.S. Shumovsky, and Tran Quang, J. Phys. A **21**, 119 (1988); V.F. Cheltsov, Opt. Acta **33**, 33 (1986).
[17] A.S. Shumovsky and Tran Quang, Phys. Lett. A **132**, 164 (1988).
[18] G.S. Agarwal, A.C. Brown, L.M. Narducci, and G. Vetri, Phys. Rev. A **15**, 1613 (1977).
[19] M. Kozierowski, S.M. Chumakov, and A.A. Mamedov, Physica A **180**, 435 (1992); M. Kozierowski, A.A. Mamedov, and S.M. Chumakov, Phys. Rev. A **42**, 1762 (1990); M. Kozierowski, S.M. Chumakov, J. Swiatlowski, and A.A. Mamedov, *ibid.* **46**, 7220 (1992).
[20] R. Dicke, Phys. Rev. **93**, 99 (1954).
[21] M. Tavis and F.W. Cummings, Phys. Rev. **170**, 379 (1968).
[22] D.F. Walls and R. Barakat, Phys. Rev. A **1**, 446 (1970).
[23] M.E. Smithers and E.Y.C. Lu, Phys. Rev. A **9**, 790 (1974).
[24] F. Persico and G. Vetri, Phys. Rev. A **12**, 2083 (1975).
[25] G. Scharf, Helv. Phys. Acta **43**, 806 (1976).
[26] R. Bonifacio and G. Preparata, Phys. Rev. A **2**, 336 (1970).
[27] S. Kumar and C. L. Mehta, Phys. Rev. A **21**, 1573 (1980).
[28] S.S. Hassan, M.S. Abdalla, A.-S.F. Obada, and H.A. Batarfi, J. Mod. Opt. **40**, 1351 (1993).
[29] S.M. Chumakov, A.B. Klimov, and J.J. Sanchez-Mondragon, Phys. Rev. A **49**, 4972 (1994).
[30] J. Gea-Banacloche, Phys. Rev. A **44**, 5913 (1991).
[31] A.Ṡ. Shumovsky and B. Tantar, Phys. Lett. A **182**, 411 (1993).
[32] V.P. Karassev, J. Sov. Laser Res. **13**, 188 (1992); V. P. Karassev, Teor. Mat. Fiz. **95**, 3 (1993); V.P. Karassev, A.B. Klimov, Phys. Lett. A **191**, 117 (1994).
[33] E.T. Jaynes and F.W. Cummings, Proc. IEEE **51**, 89 (1963).
[34] J.H. Eberly and K. Wodkiewicz, J. Opt. Soc. Am. **67**, 1252 (1977).
[35] D. Meschede, H. Walther, and G.M. Muller, Phys. Rev. Lett. **54**, 551 (1985); H. Moya-Cessa, V. Buzek, and P.L. Knight, Opt. Commun. **85**, 267 (1991).
[36] Y. Zhu, D.J. Gauthier, S.E. Morin, Q. Wu, H.J. Carmichael, and T.W. Mossberg, Phys. Rev. Lett. **64**, 2499 (1990).
[37] G.S. Agarwal, Phys. Rev. Lett. **53**, 1732 (1984).
[38] W. Lange and H. Walther, Phys. Rev. A **48**, 4551 (1993); G.S. Agarwal, W. Lange, and H. Walther, *ibid.* **48**, 4555 (1993).